AAAS
Research
Volume 2019, Article ID 4756025, 9 pages
https://doi.org/10.34133/2019/4756025

Research
A SCIENCE PARTNER JOURNAL

Research Article

Chiral Autoamplification Meets Dynamic Chirality Control to Suggest Nonautocatalytic Chemical Model of Prebiotic Chirality Amplification

Evgenii P. Talsi,[1,2] Anna A. Bryliakova,[2] Roman V. Ottenbacher,[1,2] Tatyana V. Rybalova,[1,3] and Konstantin P. Bryliakov[1,2]

[1]*Novosibirsk State University, Pirogova 2, Novosibirsk 630090, Russia*
[2]*Boreskov Institute of Catalysis, Pr. Lavrentieva 5, Novosibirsk 630090, Russia*
[3]*Vorozhtsov Novosibirsk Institute of Organic Chemistry, Pr. Lavrentieva 9, Novosibirsk 630090, Russia*

Correspondence should be addressed to Konstantin P. Bryliakov; bryliako@catalysis.ru

Received 30 July 2019; Accepted 16 September 2019; Published 4 November 2019

Oxidative kinetic resolution of 1-phenylethanol in the presence of manganese complexes, bearing conformationally nonrigid *achiral bis*-amine-*bis*-pyridine ligands, in the absence of any exogenous chiral additives, is reported. The only driving force for the chiral discrimination is the small initial enantiomeric imbalance of the scalemic (nonracemic) substrate: the latter dynamically controls the chirality of the catalyst, serving itself as the chiral auxiliary. In effect, the *ee* of 1-phenylethanol increases monotonously over the reaction course. This dynamic control of catalyst chirality by the *substrate* has been unprecedented; a consistent kinetic model for this process is presented. The reported catalyzed substrate self-enantioenrichment mechanism is discussed in relation to the problem of prebiotic chirality amplification.

1. Introduction

The origin of chirality in living systems has been debated since the time of Pasteur. Today the early assumption of Terent'ev and Klabunovskii that "life cannot and never could exist without molecular dissymmetry" [1] has become widespread, with the further realization that absolute chiral homogeneity is essential for the existence of life [2]. Moreover, it has been hypothesized that the chiral purity observed in the biosphere was achieved at the stage of prebiotic evolution and was a necessary condition for the subsequent development of self-replication characteristic of living matter [3]. These considerations put forward an abiotic and not a biotic mechanism as the primordial origin of chirality and chiral homogeneity—whether on Earth or elsewhere in the universe [2].

The question remains how the initial prebiotic enantiomeric imbalance could come about on Earth [2, 3]; existing hypotheses invoke either stochastic processes (operated by "chance," without chemical or physical directing forces) or determinate processes (directed by external chiral forces) [4–9], or assume extraterrestrial chirality protosource [10] without considering the problem in essence. However, regardless of the origin of this initial (likely small) enantiomeric imbalance, there should be an efficient mechanism of *ee* amplification, transforming the slightly nonracemic mixture of reactants into an enantiomerically enriched, ideally single-handed state. Crucially, such mechanism should not require assistance of other nonracemic chiral substances (e.g., catalysts), since simultaneous emergence of two different chirality protosources (on Earth), capable of readily reacting with each other, should be a less likely event. Asymmetric autocatalysis has been widely invoked when considering the problem of the origin of biological homochirality from the chemical perspective [11–14]. The autocatalytic Soai et al. reaction [15] provided one model for the scenario described above: the possibility of reproducible amplification of negligibly small enantiomeric imbalance (down to $5 \bullet 10^{-5}$%*ee*) has been established in this reaction [16].

On the other hand, hypothetical chemical mechanisms of chirality amplification should not necessarily be autocatalytic, mediated by the chiral reaction product. The applicability

Table 1: Kinetic resolution of scalemic 1-phenylethanol in the presence of Mn complexes **1-3**[a].

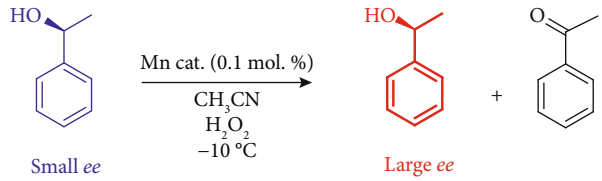

No.	Substrate	Initial *ee* (%)[b]	S_0, M	Catalyst	Conversion (%)[b]	Final *ee* (%)[b]	Kinetic parameters	
							A, M^{-1}	B, M^{-1}
1	(*S*)-1-Ph-ethanol	8.3	0.29	**1**	98.4	26.0	34.5	13.8
2	(*S*)-1-Ph-ethanol	13.0	0.29	**1**	97.3	42.6	35.0	12.5
3	(*S*)-1-Ph-ethanol	15.7	0.29	**1**	99.6	50.0	34.0	12.5
4	(*S*)-1-Ph-ethanol	8.0	0.27	**2**	85.9	16.9	66.7	31.5
5	(*S*)-1-Ph-ethanol	11.4	0.29	**2**	93.6	25.1	62.1	31.0
6	(*S*)-1-Ph-ethanol	19.5	0.30	**2**	98.9	46.8	58.3	29.2
7	(*R*)-1-Ph-ethanol	19.3	0.32[c]	**1**	97.9	49.9	33.0	14.0
8	(*R*)-1-Ph-ethanol	19.5	0.31[c]	**2**	97.5	45.3	60.5	31.5
9	(*S*)-1-Ph-ethanol	12.8	0.29	**3**	69.5	12.6	—	—
10	(*R*)-Methyl mandelate	17.4	0.20 [c]	**1**	26.3	17.5	—	—
11	(*R*)-Butyl mandelate	14.6	0.22 [c]	**1**	52.8	14.9	—	—
12	(*S*)-1-Ph-ethanol	45.5	0.36	**1**	95.7	81.2	32.5	13.7

[a]For reaction conditions, see SI. [b]Determined by chiral HPLC. [c]Initial concentration of (*R*)-enantiomer.

of kinetic resolution to the problem of enantiomeric enrichment was emphasized in a fundamental review [17], yet previously known examples of kinetic resolutions were concluded to require contrived experimental conditions, making them prebiotically unrealistic [18].

At the same time, the possibility of the reaction *substrate* itself being the raw material whose mirror symmetry was initially broken could be considered. Such substrate with small enantiomeric imbalance, which came to be in the prebiotic soup, could direct its own kinetic resolution, catalyzed by third substance(s), assembled from achiral reactants available from the primitive environment. Herewith, experimental model of such scenario based on the self-directed oxidative kinetic resolution of scalemic 1-phenylethanol is presented. It has been demonstrated that for the kinetic resolution to take place, the catalyst chirality should not be compulsorily predetermined by the chiral, enantiomerically pure ligand. The process is efficiently conducted by stereolabile manganese complexes bearing achiral tetradentate ligands; the catalyst chirality is dynamically determined by coordination of the chiral substrate to the Mn active sites.

2. Results and Discussion

2.1. Kinetic Resolution of Scalemic 1-Phenylethanol in the Presence of Complexes 1 and 2. In this work, it has been found that Mn complexes **1** and **2** (Figure 1), bearing *achiral* ligands, efficiently catalyze the oxidation of 1-phenylethanol with aqueous H_2O_2, using 0.1 mol.% catalyst loading (Table 1). The oxidation of the *sec*-alcohol to the

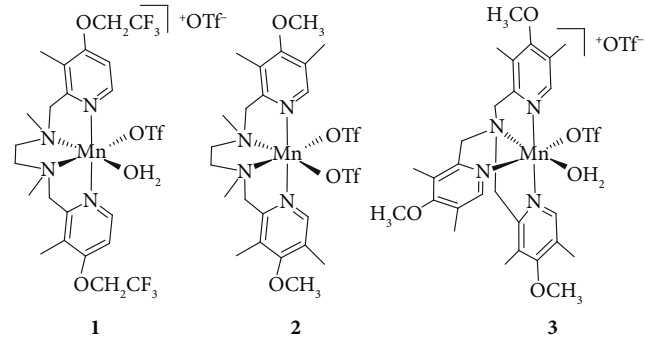

Figure 1: Structures of Mn complexes **1-3**.

corresponding ketone proceeds with very high selectivity, affording no detectable side products (SI, pages 26-48), so the amount of the residual alcohol (Figures 2 and 3) can be calculated as (100% – %conversion) with high accuracy.

Crucially, the small initial enantiomeric excess of scalemic substrate of ca. 8% *ee* ((*S*)-configuration) has been shown to increase up to 17-26% *ee* (entries 1 and 4 of Table 1). When 1-phenylethanol with higher initial enantiomeric excess was taken to the oxidation, the *ee* growth was steeper, and the final *ee* was higher (cf. entries 1-3 and 4-6 and 12). When racemic 1-phenylethanol was oxidized in the presence of **1**, no enantioenrichment was observed. The *ee* and *er* vs. conversion plots for the experiments 1-6 of Table 1 are presented in Figure 2; one can see that the enantiomeric excess grows up monotonously, this growth becoming steeper with increasing conversion.

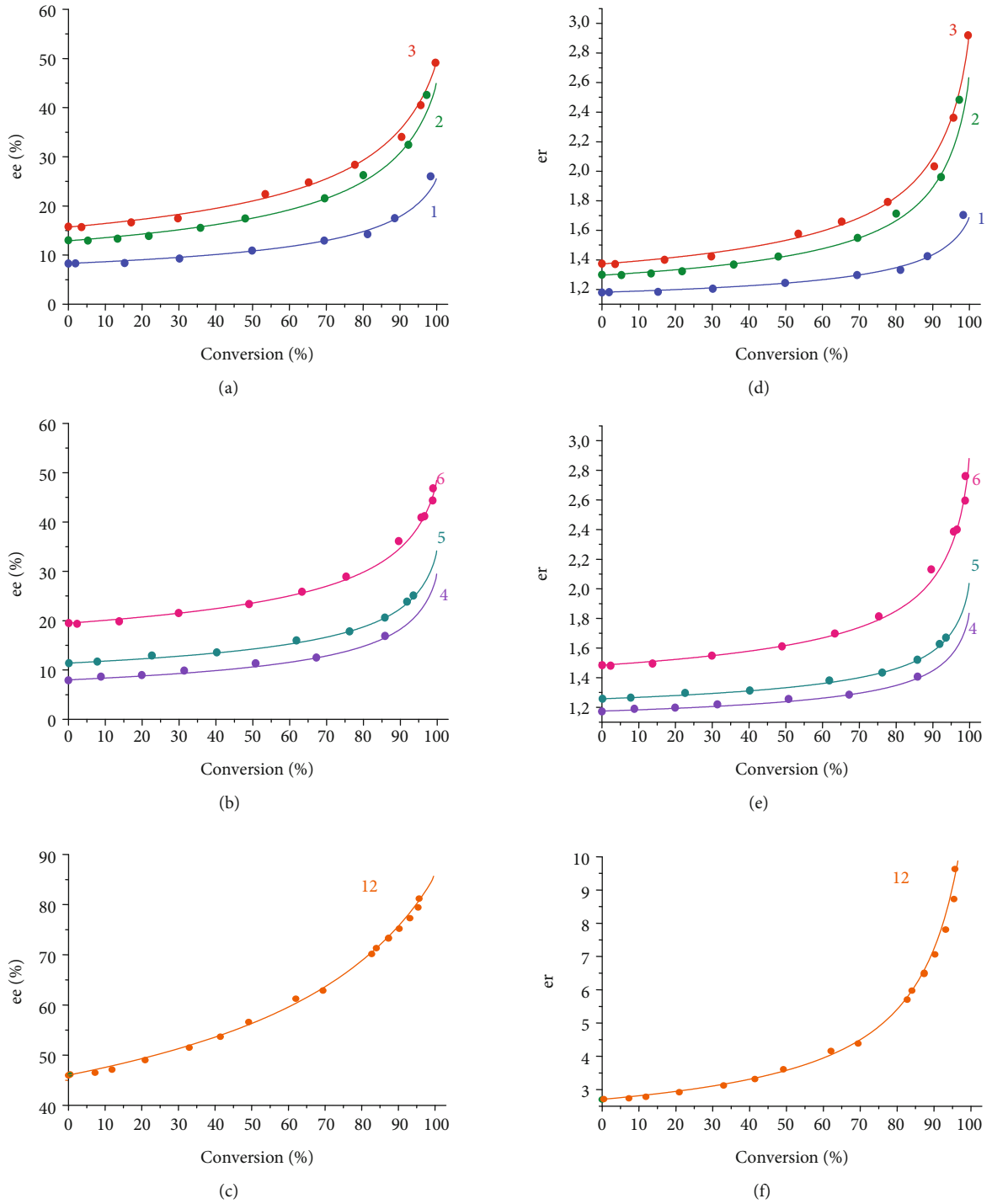

FIGURE 2: Enantiomeric excess (*ee*) vs. conversion plots for the kinetic resolution of scalemic (*S*)-1-phenylethanol in the presence of catalysts **1** (a, c) and **2** (b). Enantiomeric ratio (*er*) [S]/[R] vs. conversion plots for the kinetic resolution of scalemic 1-phenylethanol in the presence of achiral catalysts **1** (d, f) and **2** (e). Dots represent experimental data; solid lines are theoretical curves with parameters *A* and *B* given in Table 1. Curve numbers correspond to the numbers of entries in Table 1.

Eventual contamination of 1-phenylethanol with any catalytically active chiral species can be ruled out since (1) the oxidation did not occur in the absence of added Mn complex (**1**, **2**, or **3**) within at least 1 day at -10°C and (2) scalemic 1-phenylethanols of different origin—either synthesized ((*S*)-1-phenylethanol) or commercial ((*R*)-1-phenylethanol) showed identical results, with the only exception for the sign of chirality (Figure 3). Moreover, manganese complex **3** with achiral tripodal aminopyridine ligand also efficiently catalyzed the oxidation of scalemic 1-phenylethanol, but was unable to ensure *ee* amplification (Table 1, entry 9, Figure S4, SI). When scalemic methyl and

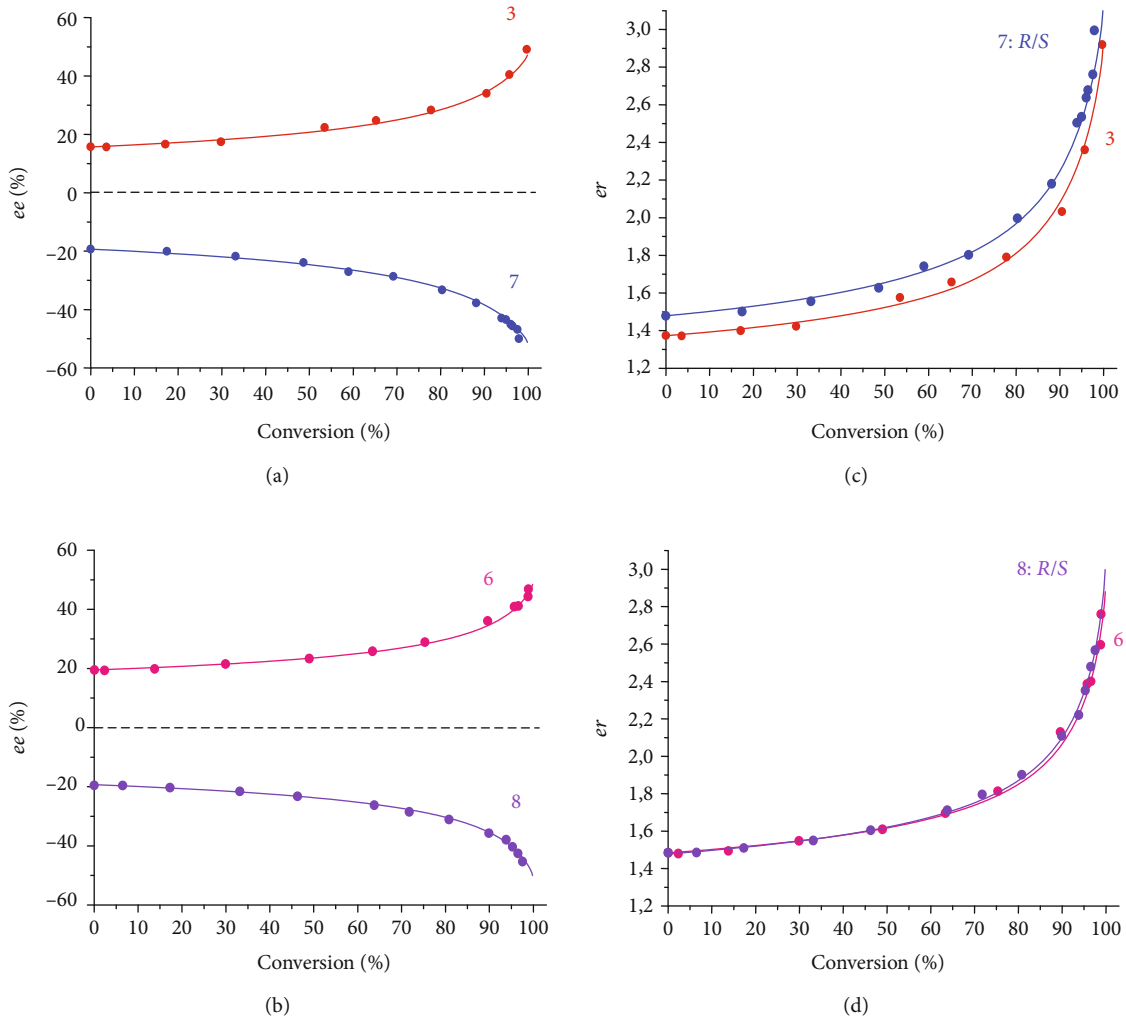

Figure 3: Enantiomeric excess (*ee*) vs. conversion plots for the kinetic resolution of scalemic (*S*)-1-phenylethanol and (*R*)-1-phenylethanol in the presence of catalysts **1** (a) and **2** (b). Enantiomeric ratio (*er*: [S]/[R] for (*S*)-substrate or [R]/[S] for (*R*)-substrate) vs. conversion plots for the kinetic resolution of scalemic (*S*)-1-phenylethanol and (*R*)-1-phenylethanol in the presence of achiral catalysts **1** (c) and **2** (d). Dots represent experimental data; solid lines are theoretical curves with parameters *A* and *B* given in Table 1. Curve numbers correspond to the numbers of entries in Table 1.

butyl mandelates ((*R*)-configuration) were oxidized in the presence of complex **2**, no *ee* enhancement was observed, either (entries 10, 11, Figure S4, SI).

2.2. The Origin of 1-Phenylethanol Enantioenrichment in the Presence of Mn Complexes Bearing Achiral Ligands. These intriguing results deserve detailed discussion. The fundamental difference between complexes **1**, **2**, and **3** is that, in contrast to the truly achiral **3**, octahedral complexes **1** and **2**, yet derived from achiral tetradentate ligands, are chiral-at-metal complexes, capable of existing in two enantiomeric forms [19, 20]. Therefore, one should first rule out the possibility of spontaneous enantioenrichment of **1** and **2** upon preparation and by-crystallization isolation. To this end, specific rotation values of **1** and **2** were measured and found to be zero, as well as, predictably, that for complex **3** (SI, Table S3).

The absence of optical rotation of the chiral-at-metal complexes **1** and **2** can indicate two alternative situations: (1) samples of **1** and **2** are conformationally stable and racemic and (2) the enantiomers of **1** and **2** are stereolabile, these complexes undergoing stereo isomerization leading to equilibrium racemic mixtures of the enantiomers. To distinguish between these possibilities, HPLC on chiral stationary phases (CSP) can be efficiently used [21–24]. To this end, HPLC conditions for the separation of enantiomeric chiral compexes (*R*,*R*)-**4** and (*S*,*S*)-**4** (Figure 4(a)) have been found: cellulose-based Chiralcel OJ-H CSP, eluent: hexane/ethanol 90 : 10, 0.1% trifluoroacetic acid, +20°C, flow rate 0.8 mL/min. Owing to the conformationally rigid bipyrrolidine backbone, the enantiomers of **4** are unable to stereo isomerize, which results in that a mixture of enantiomers gives a pair of separate, partially superimposed peaks (Figure 4(a)).

Contrariwise, the HPLC traces of complexes **1** and **2**, as well as of **3**, clearly exhibit single peaks (Figure 4(a)). While in the case of achiral **3**, such picture is predictable and unsurprising, the absence of two separate peaks from two enantiomers in the cases of **1** and **2** is highly informative,

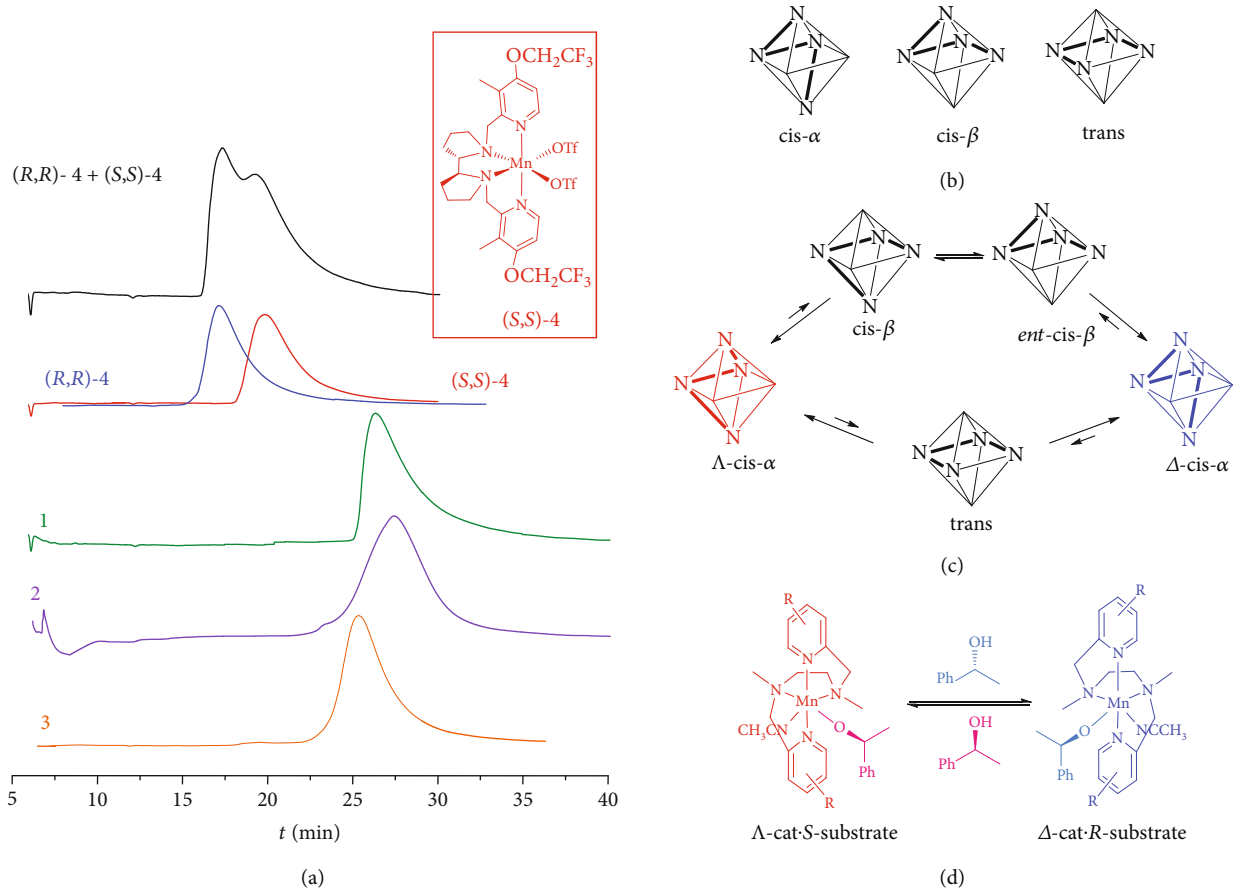

FIGURE 4: HPLC traces of (*R*,*R*)-**4** (blue), (*S*,*S*)-**4** (red), mixture (*R*,*R*)-**4** + (*S*,*S*)-**4** (black), **1** (green), **2** (violet), **3** (orange) (a). Possible topologies for octahedral iron complexes with *bis*-amine-*bis*-pyridine ligands (b). Proposed alternative pathways for the enantiomerization of complexes **1** and **2** (c). Predicted effect of enantiomers of 1-phenylethanol on the enantiomerization equilibrium (d).

characteristic of dynamic enantiomerization of these compounds. In particular, the situation of fast enantiomerization, which is much faster than the chromatographic separation, is the case, leading to the coalescence of HPLC peaks of individual enantiomers into one signal [24].

The mechanism of this stereo isomerization is key issue, directly related to the mechanism of the emergence of dynamic control of the catalyst's chirality in the course of the catalytic reaction (see below). Possible explanation may be the following. In general, three coordination topologies, such as *cis*-*α*, *cis*-*β*, and *trans* (Figure 4(b)), have been documented for octahedral iron and manganese complexes with *bis*-amine-*bis*-pyridine type ligands [25–29]. In the solid state, complexes **1** (SI), **2** [29], **3** (SI), and **4** [30, 31] adopt *cis*-*α*-coordination topology. It is known, however, that octahedral metal triflate complexes with the same *bis*-amine-*bis*-pyridine ligand can exist in both *cis*-*α* and *cis*-*β* forms; these forms are stable in solution in case the chirality of the complex is predetermined by the rigid stereochemistry of the diamine backbone [26, 27].

The situation is different if the ligand contains conformationally nonrigid diamine bridge, like 1,2-ethylenediamine: the latter readily changes its conformation [32], which could entail the change of the overall ligand coordination topology in the complex. In polar media, such as aqueous acetonitrile (i.e., under catalytic conditions), as well as in ethanol-containing eluent under HPLC conditions, the triflates would be displaced from the labile *α*-coordination cites of Mn, preferentially existing in dissociated form, which is a prerequisite for the catalytic reaction to occur. At the same time, this would facilitate changing the coordination mode of the diamine-bridged chiral ligands of **1** and **2**. Apparently, a sequence of *cis*-*α*→*cis*-*β*, *ent*-*cis*-*β*→*cis*-*β*, *ent*-*cis*-*β*→*ent*-*cis*-*α* transitions, each one proceeding via consecutive dissociation/coordination of one of the pyridine moieties, could account for the plausible pathway for enantiomerization in complexes **1** and **2** (Figure 4(c)). At the same time, the hypothetic pathway through the square planar *trans*-intermediate could not *a priori* be ruled out, yet being less likely because of the need for the simultaneous dissociation of both pyridine moieties of the ligand (Figure 4(c)).

So, manganese aminopyridine complexes bearing tetradentate achiral, ethylenediamine-based ligands appear to be conformationally nonrigid likewise manganese salen [32, 33] and ruthenium salen [34] prototypes. In the cases of the cited "achiral" manganese and ruthenium salen-based catalysts, the addition of a coordinating chiral additive resulted in the emergence of asymmetric induction in oxidation and cyclopropanation reactions [32–34]. This

was explained by translation of the chirality from the externally added chiral auxiliary toward the chirality-at-metal through shifting the equilibrium between the enantiomeric conformational isomers via formation of diastereomeric catalytic species. This phenomenon is regarded as *chiral environment amplification* or *dynamic chirality control* [32–37]. In much the same way, dynamic chirality control was more recently reported for complexes of manganese with nonrigid achiral *bis*-amine-*bis*-pyridine ligands: in the presence of Boc-protected *L*-proline as the chirality source, the dynamically racemic complexes catalyzed the asymmetric epoxidation of olefins in up to 60% *ee* [29]. The unique peculiarity of the present case, however, is that the role of the chiral auxiliary, ensuring the dynamic control of the catalyst chirality (Figure 4(d), bottom), is played *by the substrate itself*.

The absence of *ee* growth in the oxidation of alkyl mandelates on catalyst **1** (entries 10 and 11 of Table 1) apparently reflects their inability (owing to relatively low electron-donor properties) to stabilize the mirror enantioconformers of **2** via formation of diastereomeric coordination complexes [32–37]. In the case of **3**, in turn, the key condition for achieving stereoselectivity—the possibility of shifting the equilibrium between two mirror conformers of the catalyst—cannot be fulfilled in principle because of the absence of enantiomeric conformations for this complex.

2.3. Model Kinetic Scheme. The proposed reaction scheme is presented in Scheme S1, SI. For satisfactory quantitative description of the reactions in the system, the following minimal kinetic model can be considered (Figure 5). Based on DFT calculations data (SI), only the existence of [Δ-Cat·*R*] and [Λ-Cat·*S*] adducts should be taken into account, while formation of [Λ-Cat·*R*] and [Δ-Cat·*S*] adducts could be neglected as a first approximation.

Assuming the enantiomerization of the free catalyst to be the fastest reaction of all, one can obtain (see SI for details):

$$\frac{d[S]}{d[R]} = \frac{k[S] + Kk^{R}{}_{S}[R][S] + Kk^{S}{}_{S}[S][S]}{k[R] + Kk^{S}{}_{R}[S][R] + Kk^{R}{}_{R}[R][R]}, \quad (1)$$

where $k = k^{\Delta}{}_{R} + k^{\Lambda}{}_{R} = k^{\Delta}{}_{S} + k^{\Lambda}{}_{S}$ (SI). Applying evident relationships $k^{S}{}_{R} = k^{R}{}_{S}$ and $k^{S}{}_{S} = k^{R}{}_{R}$, and replacing $s = [S]/S_0$ and $r = [R]/R_0$ (R_0 and S_0 are the initial concentrations of the substrate (*R*)- and (*S*)-enantiomers), equation (1) can be reduced (SI) to the following:

$$\frac{ds}{dr} = \frac{s + AS_0(R_0/S_0)sr + BS_0s^2}{r + AS_0sr + BS_0(R_0/S_0)r^2}, \quad (2)$$

where $A = Kk^{R}{}_{S}/k = Kk^{S}{}_{R}/k$ and $B = Kk^{S}{}_{S}/k = Kk^{R}{}_{R}/k$. Equation (2) includes the initial concentration S_0 and initial enantiomeric ratio R_0/S_0, and two parameters, *A* and *B*, that can be fitted to the experimental curves (Figures 2 and 3). In Figures 2 and 3, the experimentally determined *ee* vs. conversion and *er* vs. conversion plots for entries 1-8 of Table 1 are presented, together with the theoretical dependencies

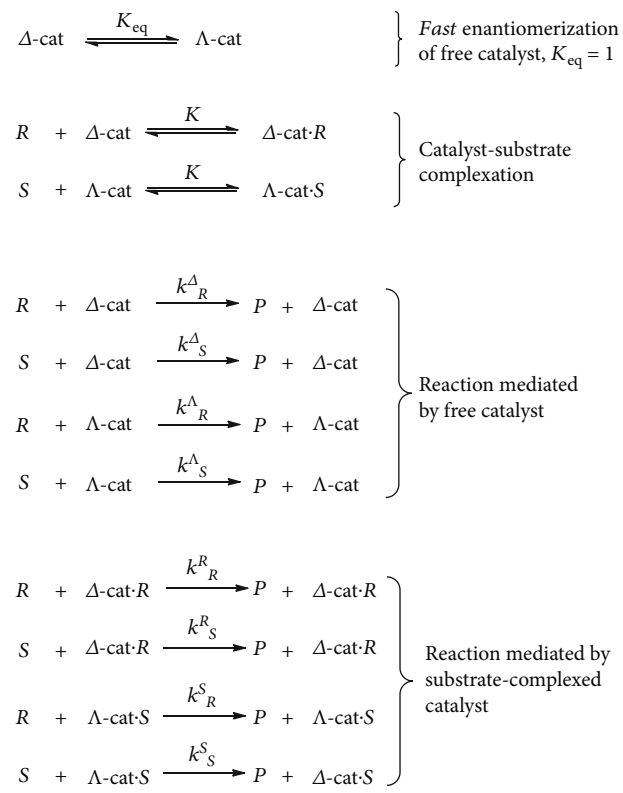

Figure 5: Proposed scheme of kinetic resolution with dynamically racemic catalyst. *P* is the product, Λ-cat and Δ-cat are the enantioconformations of the catalyst, and *R* and *S* stand for the substrate enantiomers.

according to equation (2). The values of parameters *A* and *B* resulting therefrom are given in the last two columns of Table 1. Based on the results of three separate experiments at different ee_0 for each catalyst (entries 1-3 and 4-6, respectively), the following average parameter values were calculated (1) for **1**: $A = 34.5 \pm 0.5\ M^{-1}$, $B = 12.9 \pm 0.8\ M^{-1}$ and (2) for **2**: $A = 62 \pm 4$, $B = 30.6 \pm 1.2$ (standard deviations are given). The *ee* and *er* vs. conversion plots for entries 1-3 of Table 1, simulated using the average *A* and *B* values, can be found in Figure S1, SI.

We notice that parameter AS_0 reflects the dominance of the heterochiral catalytic reaction mediated by substrate-complexed catalyst over the reaction mediated by free catalyst, while the ratio $A/B = k^{S}{}_{R}/k^{S}{}_{S} = k^{R}{}_{S}/k^{R}{}_{R}$ defines the relative rates of the heterochiral and homochiral oxidation reactions, mediated by the substrate-complexed catalyst. As compared with **1**, complex **2** shows somewhat higher *A* and *B*, ensuring higher degree of substrate-induced acceleration of the overall process; at the same time, the *A*/*B* ratio for **1** is higher than for **2** (2.7 vs. 2.0), thus witnessing better stereodiscrimination by the substrate-complexed catalyst **1**.

Upon increasing the concentration of the reaction mixture, the nonlinear amplification of *ee* and *er* with increasing conversion became steeper, and higher optical purities were achieved at comparable conversion levels (Figure S2; see also Table S1 for details). Increasing or decreasing the

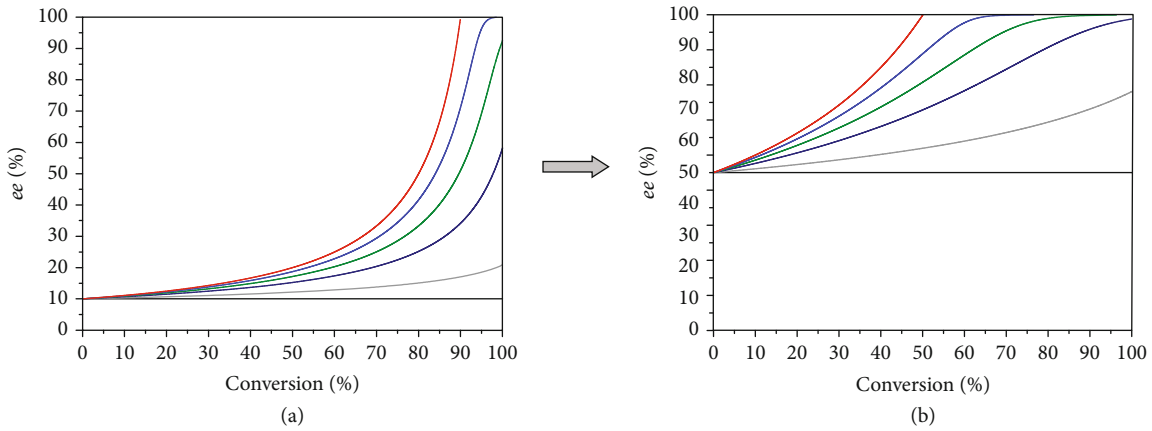

FIGURE 6: Theoretically predicted enantiomeric excess vs. conversion plots for at different initial *ee*s: ee_0 = 10% (a), ee_0 = 50% (b). S_0 = 0.30 M, $B = 10\ M^{-1}$. $A/B = 1$ (black), 2 (grey), 5 (navy), 10 (green), 25 (blue), and $10^4\ M^{-1}$ (red).

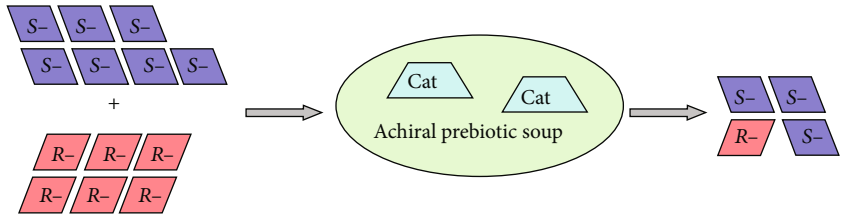

FIGURE 7: Proposed model of through-competition chirality amplification in the absence of exogenous sources of chirality. "*R*-" and "*S*-" are enantiomeric substrates; "Cat" stands for catalyst.

reaction temperature (250 and 275 K) resulted in a slight decrease of both the *A* and *B* values (see Figure S3 and Table S2 for details), thus revealing 263 K as the optimal reaction temperature.

The initial enantiomeric excess ee_0 also dramatically affects the kinetic resolution. Indeed, the picture of *ee* evolution with conversion, calculated based on the scheme depicted in Figure 5, changes significantly when passing from the case with ee_0 = 10% to the case with ee_0 = 50% (Figure 6; see also SI, Figure S5A, B, C), predicting that even for moderate *A*/*B* ratios (2…5), the low *ee* of the starting precursor can be readily amplified up to nearly 100% in a sequence of kinetic resolutions. Relevant example is presented in entry 12 of Table 1 (see also Figures 2(c) and 2(f)), where enantiomeric purity of >80% *ee* was achieved starting from 45.5% initial ee_0.

3. Conclusions

Overall, the above data demonstrate that nonracemic substrate mixtures can be kinetically resolved in a catalytic process, even though the catalyst's chirality is not predetermined by a chiral ligand: herewith, such process has been efficiently conducted by stereolabile manganese complexes with achiral tetradentate ligands, with the catalysts' chirality being dynamically determined by coordination of the chiral substrate to the Mn active sites. This is the first example of simultaneous action of two effects, chiral autoamplification [38] and dynamic chirality control (of the catalyst) [32–37], providing an unprecedented mechanism of chirality amplification in a far-from-equilibrium chemical system.

This reaction suggests an idea of alternative, nonautocatalytic [38] chemical mechanism of transformation of abiotic raw material with small initial enantiomeric imbalance [2, 8–14, 18, 39] into an enantiomerically pure specimen, without action of catalysts with predetermined chirality or participation of any other exogenous chiral molecules (Figure 7). In this system, the predominant enantiomer of the scalemic substrate itself controls the absolute configuration of the conformationally flexible catalyst, eventually "outcompeting" the other enantiomer in the concurrent catalyzed oxidation reaction. This through-competition "chemical evolution" mechanism, recreated here at the molecular level, has analogy with the natural selection-based biological evolution. Last but not least, the reported catalyzed self-enantioenrichment mechanism shows unprecedented capacity of operating efficiently and unidirectionally in partially aqueous medium [40], i.e., one step closer to the conditions modeling the prebiotic broth. Further studies of this interesting reaction are underway.

Least of all this first demonstration of the substrate-governed kinetic resolution on catalysts derived from achiral precursors claims to give exhaustive explanations, rather serving as a proof of new principle, which contributes to the discussion on the origins of homochirality on Earth by providing a so far missing piece of the overall

puzzle. Hopefully, such fresh vision of the problem can help us to make another step towards the understanding of the origins of life and its fundamental principles.

4. Materials and Methods

4.1. Materials. For catalytic epoxidation experiments, 30% analytical grade aqueous H_2O_2 was used. Mn complexes **2** [21], **4** [30, 31], and (*S*)-1-phenylethanol [30] were prepared as described. All chemicals and solvents were from Sigma-Aldrich, Acros Organics, or Alfa Aesar commercial reagents (and were used without additional purification unless noted otherwise), or were prepared according to literature procedures.

4.2. Methods. ^1H and ^{13}C NMR spectra were measured on Bruker Avance 400 at 400.13 and 100.613 MHz, respectively, or on Bruker DPX-250 at 250.13 and 62.903 MHz, respectively. Chemical shifts were internally referenced to tetramethylsilane. Specific rotation values (in CH_3CN) were measured using Kruss Optronic polarimeter P8000-T using 100 mm cuvette.

Analytical chiral resolutions were performed by HPLC on Shimadzu LC-20 chromatograph equipped with chiral stationary phases Chiralcel/Chiralpak.

Experimental (kinetic) data were treated using Origin 9.0 package.

Conflicts of Interest

The authors declare no competing financial interest.

Authors' Contributions

KPB designed the project, developed the kinetic scheme, and wrote the paper. RVO conducted the syntheses and catalytic experiments. TVR performed the X-ray measurements. AAB did DFT calculations. EPT made literature search and discussed the results.

Acknowledgments

The authors thank the Ministry of Science and Higher Education of the Russian Federation (projects AAAA-A17-117041710080-4 and AAAA-A17-117041710078-1). RVO and KPB acknowledge financial support from the Russian Foundation for Basic Research, grant 18-33-20078. AAB thanks the Siberian Supercomputer Center SB RAS. In this study, the equipment of the Center of Collective Use "National Center of Catalysis Research" and of the Multi-Access Chemical Service Center has been used.

Supplementary Materials

Supplementary materials such as detailed description of materials used; methods; synthetic, analytical, and catalytic procedures; crystal data for the new complexes **1** and **3**; treatment of the kinetic scheme presented in Figure 5; DFT calculation details; additional tables and figures related to this article; and HPLC traces can be found, in the online version, at doi:10.34133/2019/4756025. X-ray crystallographic data in CIF for CCDC 1887476 (**1**) and CCDC 1887477 (**3**) can be obtained free of charge from the Cambridge Crystallographic Data Centre via ww.ccdc.cam.ac.uk/data_request/cif and from the authors. *(Supplementary Materials)*

References

[1] A. P. Terent'ev and E. I. Klabunovskii, "The role of dissymmetry in the origin of living material," in *The Origin of Life on Earth*, pp. 95–105, Pergamon Press, 1957.

[2] W. A. Bonner, "The origin and amplification of biomolecular chirality," *Origins of Life and Evolution of the Biosphere*, vol. 21, no. 2, pp. 59–111, 1991.

[3] V. I. Gol'danskii and V. V. Kuzmin, "Chirality and cold origin of life," *Nature*, vol. 352, no. 6331, p. 114, 1991.

[4] E. I. Klabunovskii, "Homochirality and its significance for biosphere and the origin of life theory," *Russian Journal of Organic Chemistry*, vol. 48, no. 7, pp. 881–901, 2012.

[5] M. Gleiser and S. I. Walker, "Life's chirality from prebiotic environments," *International Journal of Astrobiology*, vol. 11, no. 4, pp. 287–296, 2012.

[6] M. Wu, S. I. Walker, and P. G. Higgs, "Autocatalytic replication and homochirality in biopolymers: is homochirality a requirement of life or a result of it?," *Astrobiology*, vol. 12, no. 9, pp. 818–829, 2012.

[7] R. R. E. Steendam, J. M. M. Verkade, T. J. B. van Benthem et al., "Emergence of single-molecular chirality from achiral reactants," *Nature Communications*, vol. 5, no. 1, p. 5543, 2014.

[8] C. Dressel, T. Reppe, M. Prehm, M. Brautzsch, and C. Tschierske, "Chiral self-sorting and amplification in isotropic liquids of achiral molecules," *Nature Chemistry*, vol. 6, no. 11, pp. 971–977, 2014.

[9] J. Sun, Y. Li, F. Yan et al., "Control over the emerging chirality in supramolecular gels and solutions by chiral microvortices in milliseconds," *Nature Communications*, vol. 9, no. 1, p. 2599, 2018.

[10] J. R. Cronin and S. Pizzarello, "Enantiomeric excesses in meteoritic amino acids," *Science*, vol. 275, no. 5302, pp. 951–955, 1997.

[11] K. Soai, T. Shibata, and I. Sato, "Enantioselective automultiplication of chiral molecules by asymmetric autocatalysis," *Accounts of Chemical Research*, vol. 33, no. 6, pp. 382–390, 2000.

[12] B. L. Feringa and R. A. Van Delden, "Absolute asymmetric synthesis: the origin, control, and amplification of chirality," *Angewandte Chemie International Edition*, vol. 38, no. 23, pp. 3418–3438, 1999.

[13] K. Mikami and M. Yamanaka, "Symmetry breaking in asymmetric catalysis: racemic catalysis to autocatalysis," *Chemical Reviews*, vol. 103, no. 8, pp. 3369–3400, 2003.

[14] K. Ruiz-Mirazo, C. Briones, and A. de la Escosura, "Prebiotic systems chemistry: new perspectives for the origins of life," *Chemical Reviews*, vol. 114, no. 1, pp. 285–366, 2014.

[15] K. Soai, Y. Shibata, H. Morioka, and K. Choji, "Asymmetric autocatalysis and amplification of enantiomeric excess of a chiral molecule," *Nature*, vol. 378, no. 6559, pp. 767-768, 1995.

[16] K. Soai, T. Kawasaki, and A. Matsumoto, "Asymmetric autocatalysis of pyrimidyl alkanol and its application to the study on the origin of homochirality," *Accounts of Chemical Research*, vol. 47, no. 12, pp. 3643–3654, 2014.

[17] H. B. Kagan and J. C. Fiaud, "Kinetic resolution," *Topics in Stereochemistry*, vol. 18, pp. 249–330, 1988.

[18] W. A. Bonner, "Chirality and life," *Origins of Life and Evolution of the Biosphere*, vol. 25, no. 1–3, pp. 175–190, 1995.

[19] E. C. Constable, "Stereogenic metal centres – from Werner to supramolecular chemistry," *Chemical Society Review*, vol. 42, no. 4, pp. 1637–1651, 2013.

[20] L. Zhang and E. Meggers, "Steering asymmetric Lewis acid catalysis exclusively with octahedral metal-centered chirality," *Accounts of Chemical Research*, vol. 50, no. 2, pp. 320–330, 2017.

[21] E. Yashima, "Polysaccharide-based chiral stationary phases for high-performance liquid chromatographic enantioseparation," *Journal of Chromatography A*, vol. 906, no. 1-2, pp. 105–125, 2001.

[22] C. Villani, B. Laleu, P. Mobian, and J. Lacour, "Effective HPLC resolution of [4]heterohelicenium dyes on chiral stationary phases using reversed-phase eluents," *Chirality*, vol. 19, no. 8, pp. 601–606, 2007.

[23] C. Villani, F. Gasparini, M. Pierini et al., "Dynamic HPLC of stereolabile iron(II) complexes on chiral stationary phases," *Chirality*, vol. 21, no. 1, pp. 97–103, 2009.

[24] C. Wolf, "Racemization, enantiomerization and diastereomerization," in *Dynamic Stereochemistry of Chiral Compounds: Principles and Applications*, pp. 29–135, RSC Publishing, 2007.

[25] M. Costas, A. K. Tipton, K. Chen, D. H. Jo, and L. Que, "Modeling Rieske dioxygenases: the first example of iron-catalyzed asymmetric *cis*-dihydroxylation of olefins," *Journal of the American Chemical Society*, vol. 123, no. 27, pp. 6722-6723, 2001.

[26] M. Costas and L. Que Jr., "Ligand topology tuning of iron-catalyzed hydrocarbon oxidations," *Angewandte Chemie*, vol. 114, no. 12, pp. 2283–2285, 2002.

[27] R. Mas-Balleste, M. Costas, T. van den Berg, and L. Que Jr., "Ligand topology effects on olefin oxidations by bio-inspired $[Fe^{II}(N_2Py_2)]$ catalysts," *Chemistry - A European Journal*, vol. 12, no. 28, pp. 7489–7500, 2006.

[28] R. V. Ottenbacher, D. G. Samsonenko, E. P. Talsi, and K. P. Bryliakov, "Highly enantioselective bioinspired epoxidation of electron-deficient olefins with H_2O_2 on aminopyridine Mn catalysts," *ACS Catalysis*, vol. 4, pp. 1599–1606, 2014.

[29] R. V. Ottenbacher, D. G. Samsonenko, E. P. Talsi, and K. P. Bryliakov, "Enantioselective epoxidations of olefins with various oxidants on bioinspired Mn complexes: evidence for different mechanisms and chiral additive amplification," *ACS Catalysis*, vol. 6, pp. 979–988, 2016.

[30] E. P. Talsi, D. G. Samsonenko, and K. P. Bryliakov, "Asymmetric autoamplification in the oxidative kinetic resolution of secondary benzylic alcohols catalyzed by manganese complexes," *ChemCatChem*, vol. 9, no. 13, pp. 2599–2607, 2017.

[31] E. P. Talsi and K. P. Bryliakov, "Autoamplification-enhanced oxidative kinetic resolution of *sec*-alcohols and alkyl mandelates, and its kinetic model," *ChemCatChem*, vol. 10, no. 12, pp. 2693–2699, 2018.

[32] T. Hashihayata, Y. Ito, and T. Katsuki, "Enantioselective epoxidation of 2,2-dimethylchromenes using achiral Mn-salen complex as a catalyst in the presence of chiral amine," *Synlett*, vol. 1996, no. 11, pp. 1079–1081, 2000.

[33] T. Hashihayata, Y. Ito, and T. Katsuki, "The first asymmetric epoxidation using a combination of achiral (salen)manganese(III) complex and chiral amine," *Tetrahedron*, vol. 53, no. 28, pp. 9541–9955, 1997.

[34] J. A. Miller, B. A. Gross, M. A. Zhuravel, W. Jin, and S. B. T. Nguyen, "Axial ligand effects: utilization of chiral sulfoxide additives for the induction of asymmetry in (salen)rutheniu-m(II) olefin cyclopropanation catalysts," *Angewandte Chemie International Edition*, vol. 44, no. 25, pp. 3885–3889, 2005.

[35] J. Balsells and P. J. Walsh, "The use of achiral ligands to convey asymmetry: chiral environment amplification," *Journal of the American Chemical Society*, vol. 122, no. 8, pp. 1802-1803, 2000.

[36] J. W. Faller, A. R. Lavoie, and J. Parr, "Chiral poisoning and asymmetric activation," *Chemical Reviews*, vol. 103, no. 8, pp. 3345–3367, 2003.

[37] P. J. Walsh, A. E. Lurain, and J. Balsells, "Use of achiral and meso ligands to convey asymmetry in enantioselective catalysis," *Chemical Reviews*, vol. 103, no. 8, pp. 3297–3344, 2003.

[38] K. P. Bryliakov, "Dynamic nonlinear effects in asymmetric catalysis," *ACS Catalysis*, vol. 9, no. 6, pp. 5418–5438, 2019.

[39] K. Soai, A. Matsumoto, and T. Kawasaki, "Asymmetric autocatalysis and the origins of homochirality of organic compounds. An overview," in *Advances in Asymmetric Autocatalysis and Related Topics*, pp. 1–30, Academic Press, 2017.

[40] V. A. Davankov, "Biological homochirality on the earth, or in the universe? A selective review," *Symmetry*, vol. 10, no. 12, p. 749, 2018.